Theory of ferromagnetism in planar heterostructures of (Mn,III)-V semiconductors

J. Fernández-Rossier and L. J. Sham
Department of Physics, University of California San Diego, 9500 Gilman Drive, La Jolla, California 92093-0319
(Received 27 June 2001; published 27 November 2001)

A density-functional theory of ferromagnetism in heterostructures of compound semiconductors doped with magnetic impurities is presented. The variable functions in the density-functional theory are the charge and spin densities of the itinerant carriers and the charge and localized spins of the impurities. The theory is applied to study the Curie temperature of planar heterostructures of III-V semiconductors doped with manganese atoms. The mean-field, virtual-crystal and effective-mass approximations are adopted to calculate the electronic structure, including the spin-orbit interaction, and the magnetic susceptibilities, leading to the Curie temperature. By means of these results, we attempt to understand the observed dependence of the Curie temperature of planar δ-doped ferromagnetic structures on variation of their properties. We predict a large increase of the Curie temperature by additional confinement of the holes in a δ-doped layer of Mn by a quantum well.

DOI: 10.1103/PhysRevB.64.235323 PACS number(s): 75.70.Cn, 75.50.Pp, 75.10.−b

I. INTRODUCTION

Interest in ferromagnetic III-V semiconductors lies both in fundamental physics and potentially useful technological applications utilizing spins.[1] The growth of $Ga_{1-x}Mn_xAs$, a ferromagnetic III-V semiconductor,[2–6] has raised the basic problems of the origin of the ferromagnetism and of the spin transport properties. In contrast to the much-studied Mn-doped II-VI materials,[7] Mn acts as an acceptor in GaAs so that $Ga_{1-x}Mn_xAs$ has free holes that are thought to be responsible for the high Curie temperature[2] T_C of 110 K for $x=0.054$. Progress in ''spintronics'' is made by the recent demonstrations of the injection of a spin-polarized current from both ferromagnetic metals[8–11] and magnetic semiconductors[12,13] into a semiconductor.

The Zener model of ferromagnetism for a bulk alloy of (III-V) semiconductors,[14,15] linking the Curie temperature with the spin susceptibility of the mobile holes, forms a framework for understanding the dependence of the ferromagnetism on various properties of the system, including the hole density and the Mn concentration. The semiconductors afford an opportunity to change the properties to affect the ferromagnetism, for example, by optical excitation of the carriers[16] and by field-effect control.[17] Engineering the band-gap profiles of planar heterostructures of the III-V semiconductors and the doping can also vary the factors influencing the ferromagnetic order. In experiments[18] in a double quantum well of $Ga_{1-x}As_xMn/Ga_{1-x}As_xAl$, the coupling between the two magnetic layers is observed to depend on both the thickness and the composition of the nonmagnetic barrier.

A different kind of planar system, the so-called digital ferromagnetic heterostructure, has been introduced by Kawakami *et al.*[19] This system consists of a sequence of atomic monolayers of $Ga_{1-x}Mn_xAs$ (with $x=0.25$ and 0.5) separated by several layers of GaAs. This δ-doping[20] structure displays a transition temperature that is a decreasing function of the distance between the magnetic layers. At the shortest distance reported, T_C is around 50 K.[19] At a large interlayer distance, the layers are decoupled and T_C reaches a value of around 35 K. Single layer samples also show ferromagnetism.[21]

In this paper we provide a theoretical framework to study ferromagnetism in planar heterostructures of ferromagnetic III-V semiconductors. The model combines the standard procedure to calculate the electronic structure of planar semiconductor heterostructures in the envelope-function formalism with a mean-field theory for the ferromagnetic state. Our goal is to understand the interplay of confinement, spin-orbit interaction, and close packing of Mn atoms in the ferromagnetic digital heterostructures. Keeping the theories of the electronic structure and ferromagnetism simple, enable us to study the effects of varying the system configurations, degree of interdiffusion, and carrier compensation. We apply the theory to calculations of the electronic structure and T_C for the case of single and multiple digital layers of $Ga_{1-x}As_xMn$ and for the additional confinement effect by a quantum well of a Mn layer. We show that the behavior of the double layer as a function of the layer separation is essentially that of more than two layers.

Our model is an extension to the case of planar heterostructures of the Zener model for bulk alloys of (III-V) ferromagnetic semiconductors.[14,15] It is convenient to express the problem of the localized spins and the carrier spins in an inhomogeneous system in terms of the density-functional theory.[22] It expresses the Curie temperature in terms of the carrier-spin susceptibility of the doped semiconductor, taking into account the spin-orbit interaction of the holes. Such an extension involves two technical refinements, compared to the bulk case. First, as confinement breaks the translational invariance along the growth axis z, the susceptibility becomes a function of two variables $\chi(z,z')$, rather than one of $(z-z')$. In order to determine T_C in a planar heterostructure we have to solve an integral equation whose kernel contains the nonlocal spin susceptibility $\chi(z,z')$. The derivation of the integral equation from the density-functional theory is given in Sec. II. Second, as explained in Sec. III, the calculation of the electronic structure of the holes in a planar heterostructure involves the solution of the self-consistent Schrödinger equation.[23] The calculation of the subbands, for the in-plane motion, is made using the Luttinger

Hamiltonian,[24] which includes the spin-orbit interaction. Our calculations address the regime in which both the Mn density c_M and the carrier density p are high. This implies that several subbands are occupied. Therefore, our calculations include *both* spin-orbit interaction and multiple subbands, in contrast with previous work.[25–28]

In Sec. IV we apply the formalism to the case of a single digital layer of $Ga_{1-x}As_xMn$ embedded in GaAs. From the calculated electronic structure for different values of the degree of compensation and the interdiffusion of the Mn, we find that the calculated T_C is an increasing function the density of holes and a decreasing function of the interdiffusion of the magnetic impurities. In Sec. V, we investigate the change in T_C as a function of the interlayer distance between two layers in order to understand the observed behavior of multilayers of Mn for different degrees of compensation and interdiffusion. Our numerical results for two layers, which are very similar to those for up to five layers, reproduce the main features of the experimental results. A remarkable result is found in Sec. VI where the calculated T_C for a digital layer inside a quantum well is found to increase dramatically by the additional quantum-well confinement, compared to just the confinement due to the Mn layer in Sec. IV. In Sec. VII we put our results in perspective and draw some conclusions.

II. DENSITY-FUNCTIONAL FORMULATION FOR MAGNETISM IN HETEROSTRUCTURES

The observed effects of ferromagnetism in Mn-doped III-V semiconductors appear to be consistent with the microscopic mechanism of indirect Mn-Mn spin interaction mediated by the mobile holes via the exchange interaction between the hole and the magnetic moment of the localized d electrons of the Mn impurity. A common model for the bulk system, which we shall adopt, consists of a quantum-degenerate gas of fermions that interact, via a contact Heisenberg exchange interaction, with the local magnetic moments of Mn. The random array of Mn impurities is replaced by a homogeneous distribution and the exchange interaction is reduced correspondingly. This procedure is dubbed the virtual crystal approximation.[7] The exchange coupling between Mn and the holes is treated in the mean-field approximation.[15]

The study of heterostructures of semiconductors δ doped with manganese, calls for an extension of the virtual crystal and mean-field approximations to an inhomogeneous distribution of Mn. We formulate the theory of magnetism of the inhomogeneous system in terms of the density-functional theory, extended to include the spin densities and to finite temperature.[22] The free energy of the system of Mn spins and holes as a functional of the density and spin-density distributions of the Mn spins and the hole carriers is separated into three contributions;

$$F = F_M + E_h + E_{hM}, \tag{1}$$

respectively, of Mn spins, the holes, and the Mn-hole interaction. The free energy of the Mn-spin system alone is

$$F_M[c_M(\mathbf{r}),\mathbf{M}(\mathbf{r})] = \int d^3r\, c_M(\mathbf{r})[f_0(\mathbf{M}(\mathbf{r})) + \tfrac{1}{2}J_M M^2(\mathbf{r})] + \tfrac{1}{2}\int d^3r \int d^3r'\, c_M(\mathbf{r})c_M(\mathbf{r}') \times \mathbf{M}(\mathbf{r})\cdot\mathbf{J}_{MM}(\mathbf{r},\mathbf{r}')\cdot\mathbf{M}(\mathbf{r}')]. \tag{2}$$

The number density of the Mn is denoted by $c_M(\mathbf{r})$ and $\mathbf{M}(\mathbf{r})$ is the spin expectation per Mn atom (in units of $\hbar$). The noninteracting part of the free energy per Mn spin is given by

$$f_0(\mathbf{M}) = k_B T\left[Mb - \ln\left\{ \frac{\sinh(S+\frac{1}{2})b}{\sinh\frac{b}{2}} \right\} \right], \tag{3}$$

where k_B is the Boltzmann constant, $S=\frac{5}{2}$ is the spin of Mn and $b=b(M)$ is related to the inverse of the usual Brillouin function

$$M = (S+\tfrac{1}{2})\coth[(S+\tfrac{1}{2})b] - \tfrac{1}{2}\coth(\tfrac{1}{2}b). \tag{4}$$

The second term in the integral of Eq. (2) takes into account only the short-range Heisenberg exchange between Mn spins. J_M has the dimension of energy. In GaAs it is believed to be antiferromagnetic.[15] The third term accounts for the long-range dipole interaction $\mathbf{J}_{MM}(\mathbf{r},\mathbf{r}')$ and is found to be negligible.

The temperature range under study is sufficiently low compared with the Fermi temperature of the holes that the hole free energy will be taken as the usual ground-state energy functional $E_h[p(\mathbf{r}),\mathbf{S}(\mathbf{r})]$,[22] where $p(\mathbf{r})$ is the hole density and $\mathbf{S}(\mathbf{r})$ the spin density. The interaction between holes is included in the Hartree approximation in the calculation of the subbands. As the density of holes is very high, the exchange and correlation potential in the local-density approximation is of minor importance.

The Mn-hole interaction term is given by

$$E_{hM}[p(\mathbf{r}),\mathbf{S}(\mathbf{r});c_M(\mathbf{r}),\mathbf{M}(\mathbf{r})] = -\int d^3r \int d^3r'\, p(\mathbf{r})u(\mathbf{r}-\mathbf{r}')[c_M(\mathbf{r}')-c_c(\mathbf{r}')] + J\int d^3r\, c_M(\mathbf{r})\mathbf{M}(\mathbf{r})\cdot\mathbf{S}(\mathbf{r}). \tag{5}$$

The first term on the right side of the equation is the attractive potential provided by the Mn donors to the holes with $u(\mathbf{r}-\mathbf{r}')$ being the Coulomb interaction. The experiment[2] shows compensation of the acceptors, which are believed to be antisite impurities. The compensating impurity concentration $c_c(\mathbf{r})$ is taken into account. The second term is the hole-spin interaction with the Mn spin, for which we use the simplest mean-field approximation. Functional terms beyond the mean field might be constructed from theory, such as, Refs. 29–31. The hole-Mn spin interaction J has the dimension of energy volume.

In the mean-field and virtual-crystal approximations, the model describes the hole carriers interacting with an effec-

tive magnetic field produced by the localized Mn impurities and vice versa. The variational result of the free-energy functional with respect to both the magnetization of the Mn impurities and the magnetization of the hole carriers shows the interdependence of the two magnetizations. Each is governed by the effective magnetic field generated by the other. They have to be determined selfconsistently. We report here only the work on the transition temperature. Theoretical finite magnetization studies are being carried out. Close to the Curie temperature, the magnetizations are small. The free energy is a quadratic functional of the two magnetizations. In a planar heterostructure with the growth axis along z, there is translational invariance along the x-y plane in the effective mass approximation so that quantities depend only on z. The free-energy functional per unit area is then

$$\begin{aligned} F[p(z),\mathbf{S}(z);c_M(z),\mathbf{M}(z)] &= F[p(z),c_M(z)]+\tfrac{1}{2}\int dz c_M(z)\left[\frac{3k_BT}{S(S+1)}+J_M\right] \\ &\times M_\alpha(z)^2+J\int dz c_M(z)M_\alpha(z)S_\alpha(z) \\ &+\tfrac{1}{2}\int dz\int dz' S_\alpha(z)K_\alpha(z,z')S_\alpha(z'). \end{aligned} \tag{6}$$

The first term $F[p(z),c_M(z)]$ is the density functional for the holes at zero magnetization including the impurity potential [E_h in Eq. (1) and second line of Eq. (5)]. Charge neutrality determines the total number of holes

$$\int_{-\infty}^{\infty} p(z)dz=\int_{-\infty}^{\infty}[c_M(z)-c_c(z)]dz. \tag{7}$$

The first quadratic term in M is the small M limit of Eq. (3). The coefficient of M^2 is the inverse susceptibility of the free Mn spins. The next term is the Mn hole exchange interaction term [last line in Eq. (5)]. The last term in (6) is the magnetic energy of the holes in the small magnetization limit.[22] The kernel of the integral, $K_\alpha(z,z')$, is the inverse of the nonlocal hole-spin susceptibility[22] χ

$$\int dyK_\alpha(z,y)\chi_\alpha(y,z')=\delta(z-z'). \tag{8}$$

For simplicity, we assume that the magnetization axis is the same in all the points of the sample. We have considered two situations, namely, the magnetization of both $M_\alpha(z)$ and $S_\alpha(z)$ pointing along the growth axis $\alpha=z$ or in plane $\alpha=x$.

Minimization of the energy functional (6) with respect to the magnetizations leads to two coupled equations for $M_\alpha(z)$ and $S_\alpha(z)$:

$$c_M(z)\left\{\left[\frac{3k_BT}{S(S+1)}+J_M\right]+JS_\alpha(z)\right\}=0, \tag{9}$$

$$\int dz'K_\alpha(z,z')S_\alpha(z')+Jc_M(z)M_\alpha(z)=0. \tag{10}$$

$M_\alpha(z)=S_\alpha(z)=0$ are always a solution, corresponding to the stable state only in the paramagnetic phase. The Curie temperature is the highest temperature at which Eqs. (9) and (10) have nonzero solutions. Elimination of $S_\alpha(z)$ from Eqs. (9) and (10) by Eq. (8) leads to an integral equation for the Curie temperature T_C

$$M_\alpha(z)c_M(z) =\frac{c_M(z)S(S+1)J^2}{3(k_BT_C+k_BT_M)}\int dz\chi_\alpha(z,z')c_M(z')M_\alpha(z') \tag{11}$$

where $k_BT_M\equiv S(S+1)J_M/3$. The factor $c_M(z)$ is left in place on both sides of the equation to signify the existence of the magetization $M(z)$ only in regions of finite $c_M(z)$. Equation (11), which relates T_C with the nonlocal spin susceptibility of the holes for a given planar heterostructure, $\chi_\alpha(z,z')$, is a generalization of the Weiss mean-field equations to inhomogeneous spin densities. Equation (11) extends Eqs. (10)–(12) of Ref. 26 to include multiple subband occupation and spin-orbit interaction.

III. NONLOCAL SUSCEPTIBILITY

The calculation of the Curie temperature for the planar heterostructure involves the solution of the integral Eq. (11), whose kernel contains the nonlocal spin susceptibility. In this section we briefly describe our calculation of the electronic structure and the nonlocal-spin susceptibility for a rather general planar heterostructure characterized by a profile of the Mn impurities $c_M(z)$, the profile of the compensating impurities $c_c(z)$ (antisites), and a band-gap profile that creates a potential for the holes $V_i(z)$.

For a given density profile, we solve the Poisson equation and obtain the electrostatic potential V_{el}, which, together with a band-gap potential $V_i(z)$, defines the effective mass Hamiltonian[23,24] for the envelope function of the holes

$$H_{\rm eff}=H_L\left(\mathbf{k},\frac{1}{i}\frac{\partial}{\partial z}\right)+V(z), \tag{12}$$

where $\mathbf{k}$ is the in-plane wave vector, $V(z)=V_i(z)+V_{el}(z)$, H_L is the standard 4×4 Luttinger Hamiltonian, with parameters γ_1, $\bar{\gamma}\equiv0.5(\gamma_2+\gamma_3)$, and $\mu\equiv0.5(\gamma_3-\gamma_2)$. We adopt the *cylindrical approximation* about the growth axis,[23] i.e., taking $\mu=0$ in the Luttinger Hamiltonian. This approximation has the advantage that $\epsilon_{\mathbf{k},\nu}$ does only depend on $k\equiv|\mathbf{k}|$. The physical properties involve angular integration over $\mathbf{k}$ about z so that the deviations from the cylindrical approximations are very small.[32]

The subbands $\epsilon_{\mathbf{k},\nu}$ and the corresponding eigenstates $\psi_{\mathbf{k},\nu}(z)$ are given by the solution of the set of four coupled second-order differential equations;

$$\sum_{m=-\frac{3}{2}}^{\frac{3}{2}}\left[H^{\rm eff}_{n,m}\left(\mathbf{k},\frac{1}{i}\frac{\partial}{\partial z}\right)+V(z)\,\delta_{n,m}\right]F_m^{\mathbf{k},\nu}(z)=\epsilon_{\mathbf{k},\nu}F_n^{\mathbf{k},\nu}(z), \tag{13}$$

where

$$[F^{\mathbf{k},\nu}_{3/2}(z),F^{\mathbf{k},\nu}_{1/2}(z),F^{\mathbf{k},\nu}_{-1/2}(z),F^{\mathbf{k},\nu}_{-3/2}(z)]=\psi_{\mathbf{k},\nu}(z) \quad (14)$$

are the four components of the wave function $\psi_{\mathbf{k},\nu}(z)$. Equation (13) is solved with the miniband $\mathbf{k}\cdot\mathbf{p}$ method.[23] We first solve the $|\mathbf{k}|=0$ case, in which the equations are decoupled into two ordinary Schrödinger equations corresponding to the light and the heavy holes. These have n_h and n_l bound states, evaluated by transforming the one-dimensional Schrödinger equation into a tridiagonal matrix eigenvalue problem that is solved numerically.[33] The $|\mathbf{k}|=0$ solutions form a basis set with the $2n_h$ states $\psi_{\nu h}(1,0,0,0)$, and $\psi_{\nu h}(0,0,0,1)$ and the $2n_l$ states $\psi_{\nu l}(0,1,0,0)$ and $\psi_{\nu l}(0,0,1,0)$. The finite $|\mathbf{k}|$ eigenergies $\epsilon_{\mathbf{k},\nu}$ and eigenstates $\psi_{\mathbf{k},\nu}(z)$ are obtained in terms of the basis set as the solutions of Eq. (13) as the $N\times N$ secular determinant problem, where $N=2(n_h+n_l)$. The hole density is given by

$$p(z)=\sum_{\nu}\int\frac{d^2k}{(2\pi)^2}f(\epsilon_{\mathbf{k},\nu})|\psi_{\mathbf{k},\nu}(z)|^2 \quad (15)$$

where $f(\epsilon)$ is the Fermi-Dirac occupation function, the Fermi level being fixed so that the charge-neutrality condition is met. The hole density $p(z)$ and the potential $V(z)$ are determined by iteration to self-consistency.

The nonlocal-spin susceptibility is then given by

$$\chi_{\alpha}(z,z')=\sum_{\nu}\int\frac{d^2k}{(2\pi)^2}\Bigg[\frac{\partial f(\epsilon_{\mathbf{k},\nu})}{\partial\epsilon_{\mathbf{k},\nu}}S^{\alpha}_{\mathbf{k},\nu,\nu}(z)S^{\alpha}_{\mathbf{k},\nu,\nu}(z') + \sum_{\nu'\neq\nu}S^{\alpha}_{\mathbf{k},\nu,\nu'}(z)\frac{f(\epsilon_{\nu}(\mathbf{k}))-f(\epsilon_{\nu'}(\mathbf{k}))}{\epsilon_{\nu}(\mathbf{k})-\epsilon_{\nu'}(\mathbf{k})} \times S^{\alpha}_{\mathbf{k},\nu',\nu}(z')\Bigg], \quad (16)$$

where $\alpha=(x,y,z)$ and the spin matrix elements are given by

$$S^{\alpha}_{\mathbf{k},\nu',\nu}(z)=\langle\psi_{\mathbf{k},\nu'}(z)|S^{\alpha}|\psi_{\mathbf{k},\nu}(z)\rangle, \quad (17)$$

where the angular brackets denote the expectation value over the spin degrees of freedom of the hole states $\psi_{\mathbf{k},\nu}(z)$. In the absence of spin-orbit interaction, the spin matrix elements would be independent of the in-plane momentum $\mathbf{k}$. Moreover, due to the interplay between the spin-orbit interaction and confinement, the nonlocal-spin susceptibility takes different values for in-plane and off-plane orientation. If the spin-orbit interaction was the only source of anisotropy, our calculation could determine the easy axis. Other sources of anisotropy, such as, shape anisotropy, are not considered in our calculation. In the calculations reported in this paper, we assume an in-plane magnetization, guided by the experimental result.[19]

IV. SINGLE DIGITAL LAYER

In this section we present the results of our calculations of the electronic structure and the Curie temperature T_C for GaAs doped with a single digital Mn layer of $(Ga_{0.5}Mn_{0.5})As$, as in the experiments. In an ideal δ doping, the Mn atoms occupy a single atomic plane. In the real system, Mn atoms undergo interdiffusion to occupy several layers. We assume that the compensating impurities are closely associated with the Mn atoms and assume their distributions to have the same shape

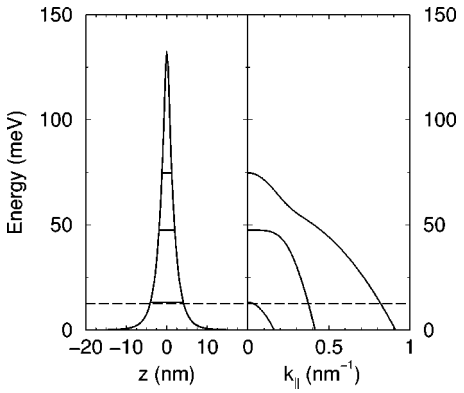

FIG. 1. Left panel: self-consistent potential for a single digital layer with $\Delta=0.5$ nm and $p=1.3\times10^{13}$ cm^{-2}, including the heavy-hole (HH) and light-hole (LH) levels. Right panel: hole subbands. The dashed line is the Fermi level.

$$\frac{c_M(z)}{\alpha_M}=\frac{c_c(z)}{\alpha_c}=\sum_n\frac{1}{\Delta}e^{-(na/\Delta)^2}\delta(z-na), \quad (18)$$

where α_c and α_M lead, respectively, to the total concentrations of Mn, c_M and of the compensating impurities c_c so that the density of holes is $p=c_M-c_c$. Hence, for a given Mn concentration c_M, a single layer is characterized by (Δ,p)

In the limit of $\Delta=0$, we recover the ideal δ-doping case, $c_M(z)=c_0\delta(z)$. Then, Eq. (11) can be solved analytically as

$$k_BT_C=\tfrac{1}{3}c_MS(S+1)J^2\chi(0,0)-k_BT_M. \quad (19)$$

The dynamics of the holes is contained in $\chi(0,0)$. We see that T_C does *not* depend on the sign of the hole Mn exchange interaction J. On the other hand, $-k_BT_M$, proportional to the direct Mn-Mn interaction, if antiferromagnetic ($J_M>0$), *decreases* the Curie temperature, as expected. In the case of a random alloy of $Ga_{1-x}As_xMn$, J_M is found negligible[15] because the distance between the Mn impurities is rather high. In contrast, the in-plane average distance between the Mn is much shorter in the digital heterostructure. However, an accurate value for both J and J_M is not known. Hereafter, we set[5] $J_M=0$ and $J=150$ meV nm^3.

In the left panel of Fig. 1 we plot the self-consistent potential for the holes corresponding to a single digital layer with $\Delta=0.5$ nm and $p=1.3\times10^{13}$ cm^{-2}, together with the energy levels for the light and the heavy holes. In the right panel we plot the subbands for the in-plane motion of the

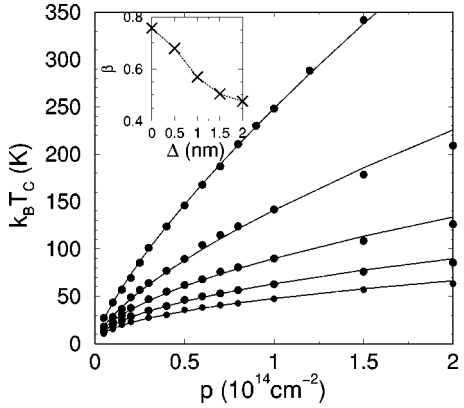

FIG. 2. T_C as a function of density of holes p for $\Delta=0$, 0.5, 1.0, 1.5 and 2.0 nm (from top to bottom). Inset: β as a function of Δ for the fit $T_C(p,\Delta)\propto p^{\beta(\Delta)}$.

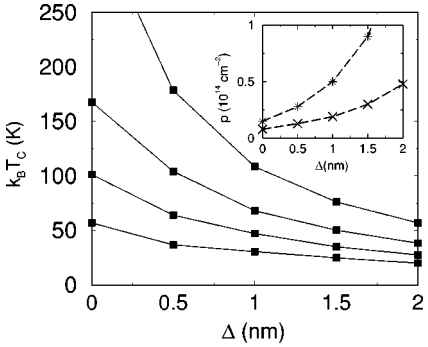

FIG. 3. T_C as a function of the interdiffusion parameter Δ for $p=1.5$ (highest), 0.6, 0.3, 0.15 (lowest) in units of 10^{14} cm^{-2}. Inset: Lines of $T_C=35$ K (crosses) and $T_C=60$ K (stars), in the (p,Δ) plane (with $J=150$ meV nm^3).

holes. The dashed line indicates the Fermi level. For $Ga_{0.5}Mn_{0.5}As$, we have $c_M=3.13\times10^{14}$ cm^{-2}. Even for a density of holes at only 4.1% of the Mn concentration, three subbands are occupied with holes. For this set of parameters the obtained T_c is 35 K the experimental value obtained by Kawakami *et al.*[19]

The spin-orbit interaction causes both the anticrossing and the nonparabolic shape of the hole subbands. As in the bulk case,[15] the spin-orbit effect also reduces significantly the effective magnetic coupling between Mn spins. Therefore, it is important to include spin orbit in the theory of ferromagnetism in planar heterostructures, an ingredient missing in previous papers for quantum wells.[25–28]

In Fig. 2 we show T_C for a single layer, as a function of the density of holes, for different values of the interdiffusion parameter Δ and for a fixed value of the Mn concentration $c_M=3.13\times10^{14}$ cm^{-2}. We take the magnetization to be in the plane of the layers in line with the experimental result.[19]For each point we have calculated the electronic structure self-consistently and solved Eq. (11) to obtain T_C. The general trend is that T_C is an *increasing* function of the density of holes. The lines are the best fit using $T_c\propto p^{\beta}$. In the inset we plot β as a function of Δ. In a two-dimensional system with parabolic bands, no spin-orbit interaction, and no Coulomb interaction, we would have obtained $\beta=0$. Remarkably, β in the single layer is even larger than the value for bulk, $\beta=1/3$.[15]

In Fig. 3 we plot T_C for the same set of single layers, as a function of Δ, for different densities of holes. The model shows that interdiffusion reduces T_C. For a fixed value of J, there is a line in the plane (p,Δ) that gives the same T_C. In the inset of Fig. 3 we plot that line for both $T_C=35$ K and $T_C=60$ K for $J=150$ meV nm^3. The first (35 K) corresponds to the Curie temperature reported by Kawakami *et al.*[19] to yield an idea of what model parameters could describe the experimental conditions. The second (60 K) has been obtained for the same kind of heterostructures grown at slightly higher temperature.[21]

The results shown in this section are calculated assuming the easy axis to be in the plane. We also have calculated T_C for a single digital layer, with $\Delta=0$ and $p>10^{13}$ cm^{-2}, assuming an off-plane easy axis. It turns out that T_c is approximately 30% higher for the the easy axis perpendicular to the plane than in the plane. Altough further work is needed to clarify this point, it is possible that other sources of anisotropy, absent in our theory, are reponsible for the observed in-plane easy axis.

V. DOUBLE DIGITAL LAYER

In this section we report on our calculations of the electronic structure and T_C for two identical digital layers, separated by N monolayers of GaAs, so that the interlayer distance is $d=N\times0.2825$ nm. Both layers are described by Eq. (18). We choose a point in the (Δ,p) parameter space, so that, for very large d, the calculated T_C is close to the experimental value of 35 K. Then we calculate $T_C(d)$ for smaller values of d.

The results are shown in Fig. 4 for two cases: ($\Delta=0.5$ nm, $p=1.3\times10^{13}$ cm^{-2}) (left panel) and ($\Delta=1.5$ nm, $p=3\times10^{13}$ cm^{-2}) (right panel). The theoretical results obtained with the first case give a better fit to the

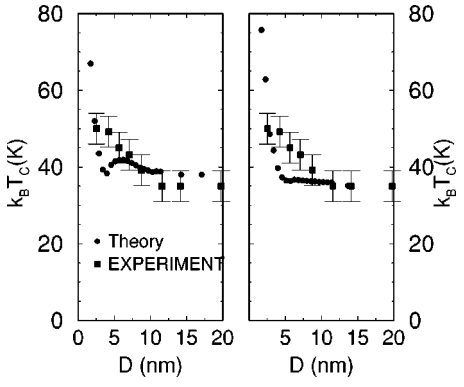

FIG. 4. Round dots: Curie temperature as a function of the interlayer distance for a double layer system. In the left panel, $\Delta=0.5$ nm and $p=1.3\times10^{13}$ cm^{-2}. In the right $\Delta=1.5$ nm and $p=3\times10^{13}$ cm^{-2}. Square dots: experimental Curie temperature for a multilayer case.[19]

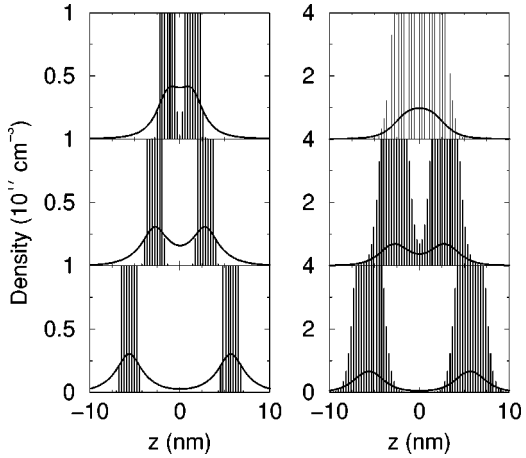

FIG. 5. Mn (shaded regions) and hole density (lines) profiles for a double layer. Left panel: $p=1.3\times10^{13}$ cm^{-2} per layer and $\Delta=0.5$ nm. Right panel: $p=3\times10^{13}$ cm^{-2} per layer and $\Delta=1.5$ nm. From top to bottom, the interlayer distance is 10, 20, and 40 monolayers.

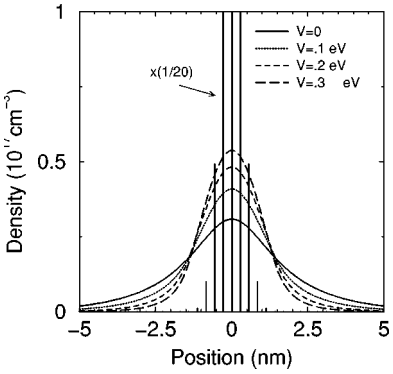

FIG. 6. Hole-density profiles for different values of the barrier potential V for a Mn digital layer (vertical lines) with $\Delta=0.5$ nm, inside a quantum well of 10 ML ($L_{QW}=2.8$ nm). The total density of holes is $p=1.3\times10^{13}$ cm^{-2}. For the sake of clarity, the Mn distribution has been divided by 20.

experimental data[19] than those obtained with the second. In Fig. 5 we plot the corresponding density profiles for three different interlayer distances to represent three regions of separation dependence in the Curie temperature. At short layer separations (upper panels of Fig. 5), both the hole and the Mn distributions overlap and T_c depends strongly on the separation d. At intermediate separations (left middle panel of Fig. 5), the two layers of Mn do not overlap but the hole distribution still does. As a result, the layers are coupled and T_C is weakly dependent on the interlayer distance. A further increase of d leads to the uncoupled regime where T_C reaches the single layer value (lower panels of Fig. 5).

Both the calculated and the measured T_C decrease as d increases and they reach a stationary value at large d. Similar behavior is obtained for several values of (p,Δ). We have also calculated T_C for three, four, and five delta layers and the separation dependence is similar. The steep decline of T_C with separation stops at interlayer distances higher than about 10 ML, the relevant experimental region. In all these cases, the theory seems to slightly *underestimate* the coupling between the layers at intermediate distances. This might indicate that the density of itinerant carriers in between the magnetic layers might be higher in the experiment than in our calculations. Further theoretical and experimental work might clarify this point.

The increase of T_C in the limit of very small D can be understood as the merger of two layers of carrier density p and Mn concentration c_M into a single layer with carrier density $2\times p$ and Mn concentration $2\times c_M$. Hence, as T_C scales linearly with both the concentration of Mn and p^β, we have $T_C(D=0)=2\times2^\beta\times T_c(D=\infty)$. For a spread $\Delta=0.5$ nm, $\beta=0.68$ and $Tc(D=0)=3.2\times T_c(D=\infty)$. The growth of a sample with interlayer distance D comparable with the interdiffusion length Δ would be very difficult due to material problems. Hence, the prediction of the theory for D smaller than 8 ML is of limited interest and is not shown in Fig. 4.

VI. DIGITAL LAYER INSIDE A QUANTUM WELL

In this section we study the electronic structure and the T_C of a single digital ferromagnetic layer inside a quantum well, using the formalism of Secs. II and III. The model predicts that the confinement effect increases T_C up to a factor of 3 compared with the unconfined single layer. The system consists of Ga_xAsAl_{1-x} barriers containing a GaAs well with a single digital layer of $Ga_{0.5}AsMn_{0.5}$ in the middle. This structure would be the ferromagnetic analog of the Be δ-doped GaAs/$Ga_{1-x}As_xAl$ quantum well.[34]

We model the interface GaAs/Ga_xAsAl_{1-x} as a barrier potential of height $V=550x$ meV. The distribution of Mn is that of Sec. IV, with $\Delta=0.5$ nm, $p=1.3\times10^{13}$ cm^{-2}. In Fig. 6 we show the distribution of holes of a 10-ML wide quantum well for different values of the aluminum content. As the

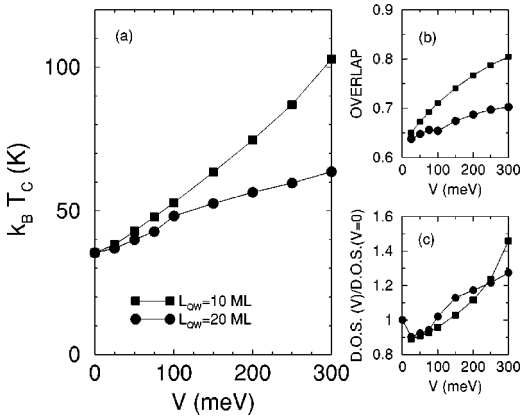

FIG. 7. (a) Curie temperature of a single digital layer, with $\Delta=0.5$ nm, $p=1.3\times10^{13}$ cm^{-2}, in a quantum well as a function of the barrier height V for two different values of the well width, $L_{QW}=10$ and 20 ML. (b) Overlap of the hole and the Mn distributions as a function of V. (c) density of states (DOS) at the Fermi level (in units of the DOS for $V=0$).

barrier potential increases, the hole distribution overlaps more the Mn layer, increasing the T_C. In Fig. 7 we plot T_C as a function of the barrier height (proportional to the Al content of the barrier), for a quantum well width of both 10 and 20 ML (2.8 and 5.7 nm) with a Mn layer in the middle of the well, with ($\Delta = 0.5$ nm, $p = 1.3 \times 10^{13}$ cm^{-2}). For the narrower well the enhancement factor can be as large as 2.9 for $V = 300$ meV, which corresponds to 54% of aluminum in the barriers. For a wider quantum well the effect is smaller.

The increase of T_C is due to two factors. The first is the increase in the overlap between the Mn and the hole distributions (see Fig. 6). In Fig. 7(b) we plot the overlap of the Mn and the hole distributions, $\int dz \sqrt{p(z) c_M(z)} / \sqrt{p c_M}$, as a function of the barrier height V. The increase of the overlap due to confinement is larger for the narrower well. The second factor is the increase of the density of states at the Fermi level (DOS). In Fig. 7(c) we plot the DOS as a function of V, normalized by the DOS at the Fermi level for the case $V = 0$. At $V = 0$ the Fermi level is close to the bottom of the second heavy hole band so that there three bands are occupied (see Fig. 1). The effect of the barrier potential is to increase the energy level spacing so that as V increases, the Fermi level goes below the second heavy-hole band and moves towards the bottom of the first light-hole band. For small values of V the DOS at the Fermi level decreases slightly, increasing up to 40% for higher values of V.

For $V > 350$ meV and $L_{QW} = 10$ nm, the Fermi level gets close to the bottom of the light-hole band where there is a dramatic increase of the DOS at the Fermi level. This leads to an even larger increase of the predicted critical temperature. Work is in progress to check if this result (not shown in the figures) remains when the finite temperature of the fermions is taken into account.

We have also checked that, for a 10-ML quantum well with a density of holes of $p = 2.5 \times 10^{13}$ cm^{-2}, the relative increase of T_C for $V = 300$ meV, is a factor of 1.8, i.e., smaller than the enhancement for $p = 1.3 \times 10^{13}$ cm^{-2}

VII. DISCUSSION AND CONCLUSIONS

The work presented in this paper is based on a model of effective-mass, virtual-crystal and mean-field approximations. A feature of the mean-field theory is that T_C scales with the square of the exchange coupling constant J.[14,15,25] We have used a value of $J = 150$ meV nm^3 from Refs. 5 and 25. However, a value three times smaller has also been reported.[35] This would change T_C by a factor of 9. In turn, this could be compensated in the theory by increasing the density of holes, including the split-off band in the calculation,[15] a larger effective mass associated with the motion in an impurity band,[36] or a direct ferromagnetic coupling J_M between the Mn atoms.

These caveats indicate the current difficulties with the theoretical prediction of the absolute values of the Curie temperature. Our model is less ambitious and is used to provide *changes* in the behavior of the Curie temperature as a function of parameters that characterize the planar heterostructure. For instance, we have presented an analysis of T_C for a single digital layer as a function of the density of compensating impurities and the spread of the Mn atoms due to interdiffusion. Our results indicate that T_C increases with the density of holes and with less interdiffusion (smaller Δ). The fact that T_C depends on density in a quasi-two-dimensional system, contrary to a naive calculation with parabolic bands, gives some theoretical support to the experiment by Ohno *et al.*[17] in which they observed a change of T_C as the density of holes changes in a $In_{1-x}As_xMn$ quantum well in a field-effect transistor. Our theory could be also applied to model ferromagnetism observed in a quantum well of *p*-doped $Cd_{1-x}Te_xMn$.[37]

In Sec. V we have presented our calculations for the double-layer system together with the experimental results for multilayers. The qualitative agreement is good, but the theory seems to underestimate the T_C at intermediate interlayer distances, i.e., the coupling between the magnetic layers is larger in the experiment than in the theory. Further work on this problem, both in the experimental characterization and in the improvement of the theory, might shed some light on the microscopic origin of ferromagnetism in this kind of systems.

In Sec. VI we have studied the confinement effects on the hole carriers that mediate the Mn-Mn magnetic coupling. This leads to a prediction of an increase of T_C by as much as a factor of almost 3, when a single digital layer is grown in a quantum-well structure. The capability to investigate the systemic changes on ferromagnetism and to predict observable effects is a strong point of the effective-mass mean-field theory.

In conclusion, we have presented a theoretical framework to calculate the electronic structure and the critical temperature of heterostructures of III-V ferromagnetic semiconductors. This work is an extension of the three-dimensional case,[15] in which the relevance of the spin-orbit interaction has been pointed out. The main features of the formalism, absent in previous papers on heterostructures, are the inclusion of several subbands, necessary because of the high density of holes in the system, and the inclusion of the spin-orbit interaction, important because it changes both the magnetic coupling and the shape of the bands. We have presented calculations of the digital magnetic heterostructures, providing a qualitative understanding of the experimental values of T_C, and we have predicted that T_C for a single digital layer can increase by a factor of 2 when embedded in a quantum well.

ACKNOWLEDGMENTS

We wish to thank Dr. D.D. Awschalom, Dr. R. Kawakami, and Dr. A. Gossard for stimulating discussions and Dr. E. Gwinn for suggesting the calculation of Sec. VII. We acknowledge financial support by Spanish Ministry of Education and by DARPA/ONR N0014-99-1-109 and NSF DMR 0099572.

[1] G. Prinz, Phys. Today **45**, 58 (1995); G. A. Prinz, Science **282**, 1660 (1998).
[2] H. Ohno *et al.*, Appl. Phys. Lett. **69**, 363 (1996).
[3] A. Van Esch *et al.*, Phys. Rev. B **56**, 13103 (1997).
[4] H. Ohno, Science **281**, 951 (1998).
[5] F. Matsukura, H. Ohno, A. Shen, and Y. Sugawara, Phys. Rev. B **57**, R2037 (1998).
[6] H. Ohno, J. Magn. Magn. Mater. **200**, 110 (1999).
[7] J. K. Furdyna, J. Appl. Phys. **64**, R29 (1988).
[8] R. Fiederling *et al.*, Nature (London) **402**, 787 (1999).
[9] A. T. Filip *et al.*, Phys. Rev. B **62**, 9996 (2000).
[10] V. P. LaBella *et al.*, Science **292**, 1518 (2001).
[11] A. Hirohata *et al.*, Phys. Rev. B **63**, 104425 (2001).
[12] Y. Ohno *et al.*, Nature (London) **402**, 790 (1999).
[13] B. T. Jonker *et al.*, Phys. Rev. B **62**, 8180 (2000).
[14] T. Dietl, A. Haury, and Y. Merle d'Aubigné, Phys. Rev. B **55**, R3347 (1997).
[15] T. Dietl *et al.*, Science **287**, 1019 (2000); T. Dietl, H. Ohno, and F. Matsukura, Phys. Rev. B **63**, 195205 (2001).
[16] S. Koshihara *et al.*, Phys. Rev. Lett. **78**, 4617 (1997).
[17] H. Ohno *et al.*, Nature (London) **408**, 944 (2000).
[18] N. Akiba *et al.*, Appl. Phys. Lett. **73**, 2122 (1998).
[19] R. K. Kawakami *et al.*, Appl. Phys. Lett. **77**, 2379 (2000).
[20] *Delta-doping of Semiconductors*, edited by E.F. Schubert (Cambridge University Press, Cambridge, 1996).
[21] R. K. Kawakami and A. Gossard (private communication).
[22] W. Kohn and L. J. Sham, Phys. Rev. **140**, A1333 (1965).
[23] D. Broido and L. J. Sham, Phys. Rev. B **31**, 888 (1985).
[24] J. M. Luttinger, Phys. Rev. **102**, 1030 (1956).
[25] T. Jungwirth, W. A. Atkinson, B. H. Lee, and A. H. MacDonald, Phys. Rev. B **59**, 9818 (1999).
[26] B. Lee, T. Jungwirth, and A. H. MacDonald, Phys. Rev. B **61**, 15606 (2000).
[27] L. Brey and F. Guinea, Phys. Rev. Lett. **85**, 2384 (2000).
[28] A. Ghazali, I. C. da Cunha Lima, and M. A. Boselli, Phys. Rev. B **63**, 153305 (2001).
[29] J. König, H. Lin, and A. H. MacDonald, Phys. Rev. Lett. **84**, 5628 (2000).
[30] M. Yang, S. Sun, and M. Chang, Phys. Rev. Lett. **86**, 5636 (2001).
[31] M. Sigrist, K. Ueda, and H. Tsunetsugu, Phys. Rev. B **46**, 175 (1992).
[32] S.-R. Yang, D. Broido, and L. J. Sham, Phys. Rev. B **32**, 6630 (1985).
[33] M. E. Lazzouni and L. J. Sham, Int. J. Comput. Math. Electr. and Elect. Eng. **14**, 129 (1995).
[34] Y. C. Shih and B. G. Streetman, Appl. Phys. Lett. **59**, 1344 (1991); J. Wagner and D. Richards, *Delta-dopings of Semiconductors* (Ref. 20), Chap. 15.
[35] T. Omiya *et al.*, Physica A **E7**, 976 (2000).
[36] R. N. Bhatt and M. Berciu, Phys. Rev. Lett. **87**, 107203 (2001).
[37] A. Haury *et al.*, Phys. Rev. Lett. **79**, 511 (1997).